Optical reflectivity measurements using a laser plasma light source

M. L. Bortz[a] and R. H. French[b]
Central Research and Development Department, E. I. duPont and de Nemours and Co., Wilmington, Delaware 19880

(Received 3 July 1989; accepted for publication 29 August 1989)

Light produced by a laser plasma light source (LPLS) is used to perform optical reflectivity measurements on single crystals from 5 to 40 eV in a single experiment. The intense continuum generated by the rare-earth plasma allows a significantly higher resolution above 15 eV and extends the measurements to higher energies than those attainable with other laboratory based light sources. This is the first application of a LPLS to vacuum ultraviolet spectroscopy of solids and we demonstrate this capability on two insulating materials, α-Al_2O_3 and $MgAl_2O_4$.

A powerful laser pulse incident on a metal surface produces a dense, high-temperature plasma. Upon relaxation the plasma emits line as well as continuum radiation, and laser plasma light sources (LPLS) yield bright time-resolved pulses extending from the visible to the soft x-ray region.[1] There has been extensive study of laser plasma generation directed at enhancing desired spectral output. In general, the choice of target material determines the balance between line and continuum emission while the laser energy and pulse width affect the intensity and duration of the plasma radiation. To date, the development of plasma light sources has focused on the production of soft x rays for pumping noble gas UV lasers,[2] lithography and microscopy applications,[3] and time-resolved gas phase fluorescence spectroscopy.[4] Yet very little effort has been directed at the vacuum ultraviolet (VUV) region relevant to electronic structure research. This may seem surprising since no conventional laboratory-based light source generates useful continuum above 15 eV. However, plasma-based light sources have poor imaging and stability properties due to ablated target material and contamination of windows, mirrors, and other optical elements, making measurements on materials very difficult. Previously demonstrated applications did not require imaging the plasma light off a solid sample or long-term source stability. However, when certain metal targets are used, plasma light sources generate line-free continuum over the range 2–50 eV, making them potentially ideal VUV light sources.[5]

In this letter we describe the first application of a LPLS to the study of the optical properties of materials. We have coupled the light from a laser-produced Samarium plasma into the optical path of a normal incidence spectrophotometer, and present absolute reflectivity measurements from 5 to 40 eV on single crystals of α-Al_2O_3, for which results over a limited energy range are available in the literature, and $MgAl_2O_4$, for which these are the first published results.

Figure 1 shows a schematic diagram of the LPLS. An 8 ns, 500 mJ, 20 Hz pulse from a Nd:YAG laser is focused by a 300 mm focal length lens to a 100 μm spot on the surface of a cylindrical Sm target rod. The laser pulse intensity is roughly 10^{12} W cm^{-2}. The rod is continuously stepped via a helical drive to ensure a clean surface for each pulse and can be surrounded by 1 Torr of either He or Ar. The gas reduces the expansion rate of the plasma leading to more intense output and order sorts the light when making measurements at longer wavelengths (He_{cutoff} = 50 nm, Ar_{cutoff} = 80 nm). The source chamber is separated from the ultrahigh vacuum (UHV) environment of the spectrometer by a differential pumping arrangement consisting of two apertures and a small intermediate chamber. The source chamber is mechanically pumped while the intermediate chamber and spectrophotometer are independently turbopumped; pressures under normal operation are 1, 10^{-4}, and 10^{-7} Torr, respectively. The first aperture is a microcapillary plate with a 50 μm pore diameter, the second aperture is an array of 1-mm-diam tubes, and each aperture has a length which yields an f number of 40. Apertures are mounted so that the pore axis can be aligned with the optical path of the spectrometer. The distance between the rod and the capillary plate is 5 cm, and the distance between the plate and the second aperture is 10 cm. This configuration eliminates Sm contamination of the spectrophotometer, as judged by a quartz crystal oscillator positioned directly above the second aperture.

Contamination of the microcapillary plate reduces the long-term stability of the plasma light, and the angular position on the Sm target rod where the plasma is produced affects the direction of the radially emitted Sm plume. As the position approaches the vertical optical path of the spectrometer, imaging efficiency increases, but Sm contamination of the microcapillary plate also increases. As the position approaches the horizontal laser beam path the opposite effects occur, and an angular position of 45° is a com-

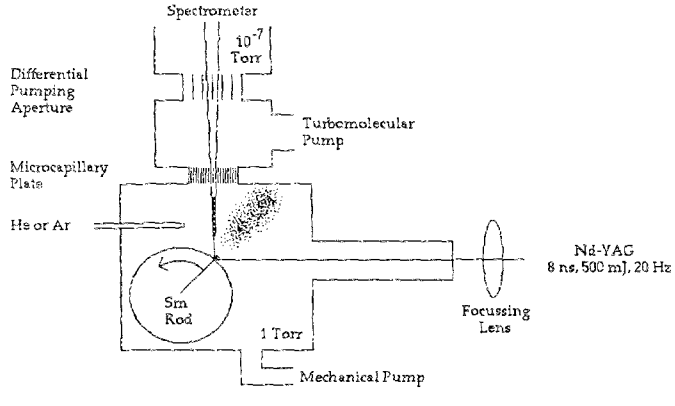

FIG. 1. Schematic diagram of the LPS.

[a] Current address: Dept. of Applied Physics, Stanford University, Stanford, CA 94305.
[b] To whom correspondence should be addressed.

 0003-6951/89/451955-03$01.00

promise between imaging efficiency and system cleanliness. Contamination of the microcapillary plate is further minimized by positioning the filter gas inlet above the Sm rod at a right angle to the optical path, deflecting the plume. While the shot-to-shot variation in plasma light intensity caused by instability in the laser pulse is roughly 5%, the average plasma intensity is very stable and allows continual operation for over 10^7 shots during which time no decrease in intensity is observed.

The cone of plasma-produced white light exits the second aperture and is focused by a spherical mirror onto either a sample or an iridium reference mirror. The spot size on the sample or reference mirror surface is estimated to be 3 mm in diameter. Details concerning the grating polychromator and detection system will be described in a future publication.[6] Briefly, the reflected component passes through a 100 μm entrance slit and is dispersed by a 1 m, normal incidence, Ir-coated, 1800 groove/mm concave diffraction grating. Detection is performed dispersively using a sodium salicylate focal plane phosphor that is fiberoptic-coupled to an image-intensified, 1024-element photodiode array with roughly single-photon sensitivity. The grating dispersion and detection optics allow data collection at 23-nm-wide intervals, with a photon flux on the order of 500 counts/shot/nm. Between 2^{14} and 2^{15} counts are necessary to obtain the signal/noise ratio in the data presented here, and a complete data set consists of 11 separate 1024 point reflectivities from both the sample and reference mirror. At a 20 Hz repetition rate, data collection for all 11 regions takes 2 h, during which no drift in the LPLS stability or alignment is detected. The determination of absolute reflectivity magnitudes requires the reflectivity of the iridium reference mirror, measured in a separate instrument. The plasma continuum coupled with this detection scheme yields a constant wavelength point resolution of 1 Å and reflectivity magnitudes reproducible from separate data sets to within $\Delta R/R = 5\%$.

Samples used in this study were Union Carbide single crystals of (0001) oriented α-Al_2O_3 and a geological sample of $MgAl_2O_4$. The choice of these materials was motivated by the increasing importance of oxide materials and the limited information about their fundamental electronic structure. Surface quality is critical for accurate reflectivity measurements and surfaces were polished with a 1 μm diamond paste followed by the removal of a minimum of 40 μm of material using a colloidal silica chemical-mechanical polish. This last step is essential to obtain accurate reflectivities without damage or strain-induced broadening.

Figure 2 shows the measured normal incidence reflectivities for Al_2O_3 and $MgAl_2O_4$ from 5 to 40 eV. The data have not been smoothed. The Al_2O_3 reflectivity exhibits an excitonic transition at 9.1 eV associated with the fundamental absorption edge, and we clearly resolve higher energy reflectivity features at 12.0, 12.9, 14.9, 17.4, 19.0, and 21.8 eV. We also observe a reflectivity peak at 32 eV which we identify as a transition from the O 2s lower valence band. Previous results from 8.5 to 28.5 eV show only a broad reflectivity band peaked at 13 and 20 eV, with no other features resolved.[7] The reflectivity for $MgAl_2O_4$ has not been previously reported. The transmission cutoff for $MgAl_2O_4$ is 7.25 eV. We observe

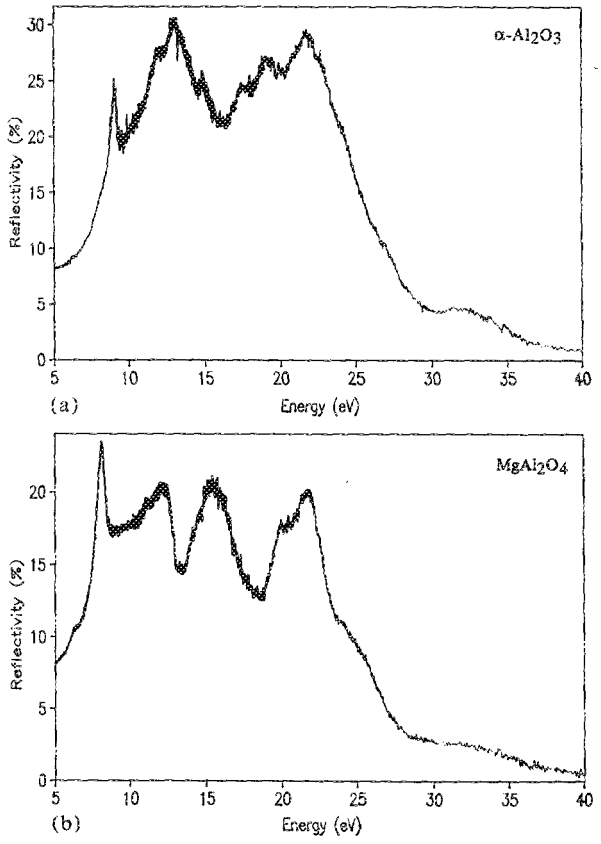

FIG. 2. Reflectivity data obtained using the LPLS, extending from 5 to 40 eV for (a) α-Al_2O_3 and (b) $MgAl_2O_4$.

impurity absorption at 6.4 eV and a large reflectivity peak at 8.1 eV, corresponding to the onset of intrinsic absorption. At higher photon energies the $MgAl_2O_4$ reflectivity shows significant structure including peaks at 12.2, 15.5, 20.0, 21.7 eV, a shoulder at 24.1 eV, and a band that extends to 35 eV. By photon energies of 40 eV, the reflectivities of both Al_2O_3 and $MgAl_2O_4$ drop to less than 1%, indicating that we have exhausted the dielectric response functions and demonstrating that the LPLS coupled to this spectrometer allows one to perform reflectivity measurements over the entire range of interband transitions in insulating materials.

Figure 3 shows the calculated optical conductivities for Al_2O_3 and $MgAl_2O_4$. The fast Fourier transform based Kramers–Kronig technique used to calculate the optical properties has been described previously.[8] As an external verification of our measurements and our calculation we have performed electron energy loss experiments on Al_2O_3 and $MgAl_2O_4$, and they agree well with peaks in the calculated $\mathrm{Im}(1/\epsilon)$, as expected from classical dielectric theory. It is important to note that (1) the LPLS allows measurements to over 40 eV, so that fundamentally the high-energy extrapolation used in the Kramers–Kronig analysis introduces a minimum error, and (2) the LPLS continuum output coupled with the dispersive detection yields a much higher energy resolution at photon energies above 15 eV than attainable with other laboratory-based light sources. Previous attempts at analysis of oxide reflectivity data were hampered by poor resolution at high energies, and modulation techniques that proved so helpful in determining the critical point structure

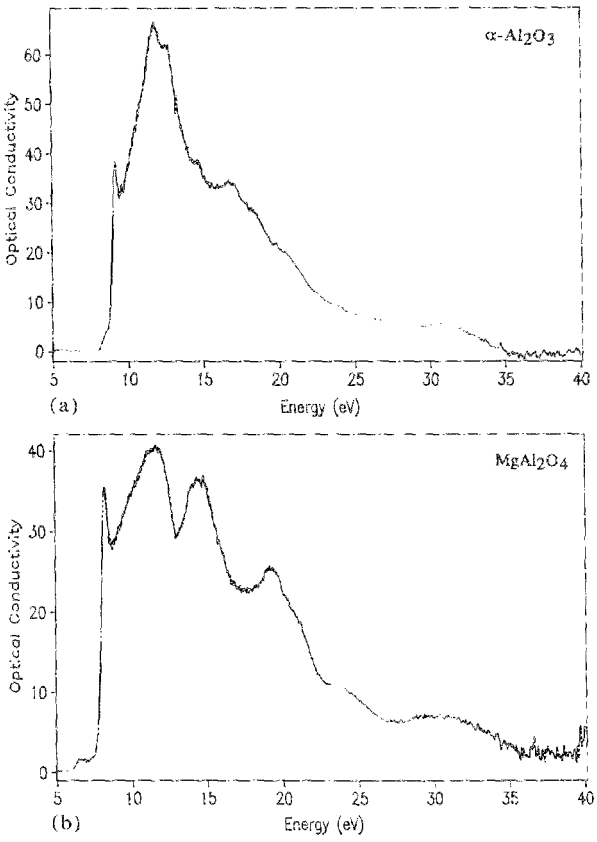

FIG. 3. Optical conductivities ($\sigma_1 = \epsilon_2 E$) for (a) α-Al_2O_3 and (b) $MgAl_2O_4$, derived from a Kramers–Kronig analysis of the reflectivity data.

of semiconductors were not applied to oxides. However, the data presented here allow a rigorous critical point analysis, and will be the subject of a future publication.[9]

While most work on laser plasma light sources focuses on the soft x-ray region, the Sm LPLS generates light throughout the UV with intensity peaking at about 50 eV before dropping off gradually.[10] Our instrument is limited to 40 eV by the normal incidence iridium reflections necessary to perform the reflectivity measurement, but the use of grazing incidence optics would allow a variety of experiments to be performed in the XUV or soft x-ray region. Furthermore, while the measurements presented here are not time-resolved, plasma light duration is limited only by the laser pump pulse and plasma relaxation processes. In general, shorter pulse, higher intensity, higher repetition rate laser pulses decrease the amount of target material contamination,[11] and we do not anticipate that any change would be necessary in the source or imaging configuration described here to perform time-resolved measurements.

The authors would like to acknowledge the assistance of R. D. Fancy and the Acton Research Corporation in the design and construction of the LPLS spectrophotometer, and M. L. Ginter in the design of the LPLS. The assistance of D. J. Jones is also greatly appreciated.

[1]K. Eidmann and T. Kishimoto, Appl. Phys. Lett. **49**, 377 (1986); O. R. Wood, II, W. T. Silfvast, H. W. K. Tom, W. H. Knox, R. L. Fork, C. H. Brito-Cruz, M. C. Downer, and P. J. Maloney, Appl. Phys. Lett. **53**, 645 (1988); M. M. Murnane, H. C. Kapteyn, and R. W. Falcone, Phys. Rev. Lett. **62**, 155 (1989); P. K. Carroll, E. T. Kennedy, and G. O. Sullivan, Appl. Opt. **19**, 1454 (1980).
[2]H. C. Kapteyn, R. W. Lee, and R. W. Falcone, Phys. Rev. Lett. **57**, 2939 (1986); H. C. Kapteyn and R. W. Falcone, Phys. Rev. A **37**, 2033 (1987).
[3]D. J. Nagel, C. M. Brown, M. C. Peckerar, M. L. Ginter, J. A. Robinson, T. J. McIlrath, and P. K. Carroll, Appl. Opt. **23**, 1425 (1984); P. Gohil, H. Kapoor, D. Ma, M. C. Pekerar, T. J. McIlrath, and M. L. Ginter, Appl. Opt. **24**, 2024 (1985); J. A. Trail, R. L. Byer, T. W. Barbee, Jr., Appl. Phys. Lett. **52**, 269 (1988).
[4]H. C. Kapteyn, M. M. Murnane, and R. W. Falcone, Opt. Lett. **12**, 663 (1987).
[5]F. B. Orth, K. Ueda, T. J. McIlrath, and M. L. Ginter, Appl. Opt. **25**, 2215 (1986).
[6]R. H. French, presented at the 9th International Conference on VUV Radiation Physics, Honolulu, HA, July, 1989, Phys. Scr. **41** (to be published).
[7]E. T. Arakawa and M. W. Williams, J. Phys. Chem. Solids **29**, 735 (1968).
[8]M. L. Bortz and R. H. French, Appl. Spectrosc. **43**, 1498 (1989).
[9]M. L. Bortz, R. H. French, D. J. Jones, R. V. Kasowski, and F. S. Ohuchi, Proceedings of the Ninth International Vacuum Ultraviolet Radiation Physics Conference, Hawaii, Phys. Scr. **41** (to be published).
[10]J. M. Bridges, C. L. Cromer, and T. J. McIlrath, Appl. Opt. **25**, 2208 (1986).
[11]M. L. Ginter and T. J. McIlrath, Appl. Opt. **27**, 885 (1988).